

Simultaneous and Sequential Presentations Differentially Modulate the Temporal Dynamics of Working Memory Processes

Ya-Ting Chen and Bo-Cheng Kuo

Abstract

■ Working memory (WM) involves continuous and dynamic processes, including encoding, maintenance, and retrieval. While many studies have focused on the maintenance of WM information, encoding strategies also impact WM performance and can be shaped by the presentation format of stimuli. However, how presentation formats modulate neural responses across WM stages remains unclear. To address this issue, we conducted an EEG study examining the effects of presentation formats (simultaneous, location-sequential, and centersequential presentation) and WM loads (one and three abstract shapes). Behavioral results showed longer RTs for the locationsequential than for the center-sequential format. Additionally, the recency effects observed in both sequential conditions reflect the influence of ordinal information. EEG results revealed distinct load-dependent alpha activity patterns across presentation formats during WM maintenance. Simultaneous

presentations exhibited a persistent decrease in alpha power, whereas both sequential presentations exhibited an initial decrease followed by a subsequent increase. During sequential encoding, alpha power decreased cumulatively with each additional item in the location-sequential format, but not in the center-sequential format. At retrieval, the probe elicited a load-dependent negative potential (i.e., the N3rs) across all formats. The N3rs load modulation was stronger for simultaneous presentations than sequential ones and was more pronounced for earlier positions than for the last position in sequential presentations. In conclusion, our findings demonstrate that the spatial and temporal order information embedded in presentation formats modulates load-dependent neural responses across WM stages. These effects extend beyond maintenance to encoding and retrieval, highlighting the influence of presentation formats on WM neural dynamics.

INTRODUCTION

Working memory (WM) retains sensory information that is no longer accessible in the external environment, enabling it to guide behaviors (D'Esposito, 2007; Miyake & Shah, 1999; Cowan, 1998; Baddeley, 1992). Extensive research has demonstrated severe limitations in WM capacity and its underlying neural mechanisms, as revealed through brain imaging techniques (Xu, 2017; Serences, 2016; D'Esposito & Postle, 2015; Stokes, 2015; Luck & Vogel, 2013). Despite significant advancements in understanding the neural correlates of WM maintenance (Sreenivasan & D'Esposito, 2019), WM encompasses continuous and dynamic processes, including encoding, maintenance, and retrieval (Jonides et al., 2008). However, the extent to which the presentation of external stimuli influences neural responses across all stages of WM processing remains unclear. In this EEG study, we investigated whether and how stimulus presentation formats modulate the neural dynamics of WM processes.

Neuroimaging evidence in humans has revealed that the representation and storage of sensory information in WM involves multiple brain regions (Christophel, Klink,

Spitzer, Roelfsema, & Haynes, 2017; D'Esposito & Postle, 2015). Studies using fMRI have shown that the perceptual attributes of mnemonic information are represented in early visual areas (Harrison & Tong, 2009; Serences, Ester, Vogel, & Awh, 2009) and encounter a storage bottleneck in the posterior parietal cortex (Xu, 2017; Bettencourt & Xu, 2016; Christophel, Hebart, & Haynes, 2012; Todd & Marois, 2004). While these findings highlight how brain regions represent and maintain WM information under capacity limitations, it is important to acknowledge that WM processes are inherently temporal and dynamic. Electrophysiological studies have assessed temporal characteristics by investigating the ERP and brain oscillations. For example, neural evidence revealed that the slow-wave negative potential (i.e., contralateral delay activity) scales with the number of memory items until reaching a plateau at higher WM loads (Luria, Balaban, Awh, & Vogel, 2016; Fukuda, Mance, & Vogel, 2015; Vogel & Machizawa, 2004). Alpha power tracks the content of perceptual information persisting throughout the maintenance period (Chen, van Ede, & Kuo, 2022; Fukuda et al., 2015).

Encoding strategies significantly influence the WM storage capacity. Factors such as task demands (Linke, Vicente-Grabovetsky, Mitchell, & Cusack, 2011) and

explicit instructions (Bengson & Luck, 2016) can influence encoding effectiveness. Individuals employing more effective encoding or filtering strategies often exhibit superior WM task performance (Unsworth, 2016; Luck & Vogel, 2013; Vogel, McCollough, & Machizawa, 2005). The format in which stimuli are presented during encoding influences task performance. Simultaneous presentation emphasizes spatial information (e.g., the spatial relationships among items within a memory array), whereas sequential presentation emphasizes ordinal information (e.g., the serial position of items in a memory list; Manohar, Pertzov, & Husain, 2017). These distinct formats can lead to varying encoding strategies in WM tasks (Chung, Brady, & Störmer, 2024; Brady & Störmer, 2022; Frick, 1985).

Although previous studies using simultaneous presentations have linked electrophysiological responses to WM load and capacity (Pavlov & Kotchoubey, 2021; Luria et al., 2016), sequential presentations provide novel insights into WM encoding and maintenance. For example, recent studies have shown that the magnitude of contralateral delay activity during WM encoding increases progressively with each additional item in the sequential presentation of memoranda, reflecting a cumulative encoding process where previously encoded items must be concurrently maintained (Pomper, Ditye, & Ansorge, 2019; Wang, Rajsic, & Woodman, 2019). However, as simultaneous presentation relies more on spatial information and sequential presentation on temporal order, the two formats differ fundamentally in nature. As a result, direct comparisons of their associated neural responses remain challenging due to differences in spatial configuration and temporal dynamics (Pavlov & Kotchoubey, 2021; Okuhata, Kusanagi, & Kobayashi, 2013).

In this study, we investigated whether and how stimulus presentation formats influence neural dynamics across WM processes. We recorded scalp EEG while participants performed WM tasks of varying presentation formats (simultaneous, location-sequential, and center-sequential presentations) and WM loads (one and three abstract shapes). This design provided a novel opportunity to investigate the effects of ordinal information derived from location-sequential presentations compared with simultaneous presentations, as well as spatial information derived from location-sequential presentations compared with center-sequential presentations (Manohar et al., 2017). Oscillatory activity in the alpha band was measured during WM encoding and maintenance (Chen et al., 2022; Fukuda et al., 2015). In addition, an ERP marker, the N3rs—specifically associated with searching for the target item within WM (Kuo, Rao, Lepsien, & Nobre, 2009; Nobre, Griffin, & Rao, 2008)—was measured during retrieval. By comparing different presentation formats, we examined the influence of spatial and ordinal information on not only the maintenance of WM but also the encoding and retrieval processes. Our results reveal that load-dependent neural modulations across WM processes vary with presentation format.

METHODS

Participants

Twenty-four healthy volunteers (13 females and 11 males, age range: 20-30 years, mean age = 24.33 years) participated in this study. The participants were right-handed, according to the Edinburgh Handedness Inventory (Oldfield, 1971); had normal or corrected-to-normal vision; and had no neurological, psychological, or physical conditions. The participants provided informed written consent prior to the experiment and were financially reimbursed for their time (\$750 NTD, approximately \$25 USD). We conducted a post hoc sensitivity analysis using the MorePower software (Campbell & Thompson, 2012), tailored to our 3 (format) \times 2 (load) within-subjects design. Assuming $\alpha =$.05 and 80% power, our sample size of 24 participants was sufficient to detect both the main effect and the interaction effect with a partial eta squared (η_p^2) of approximately .183 or larger, which corresponds to a large effect size (Cohen's $f \approx 0.47$). All experimental methods and procedures were approved by the Research Ethics Office of National Taiwan University.

Stimuli and Apparatus

We selected six abstract shapes from a set of 100 meaning-less closed-shape contours developed by Endo, Saiki, Nakao, and Saito (2003). Each stimulus subtended a visual angle of approximately $1.58^{\circ} \times 1.58^{\circ}$ (edge-to-edge). For the simultaneous and location-sequential presentations during the encoding phase, each stimulus was positioned randomly in one of three possible locations of an invisible 1×3 matrix that subtended approximately 1.58° (vertical) $\times 6.03^{\circ}$ (horizontal). For the center-sequential presentation, the stimulus was always presented at the center of the screen. All visual stimuli were gray in color and presented against a black background. The stimuli were presented on a 17-in. cathode ray tube (CRT) monitor with a refresh rate of 60 Hz using Presentation software (Neurobehavioral Systems).

Task Design

The task procedure is illustrated in Figure 1. The participants performed a delayed response WM task. The experimental design followed a 3 (presentation format: simultaneous, location-sequential, and center-sequential) \times 2 (WM load: high, low) within-subjects factorial design.

Each trial began with a centrally displayed fixation cross for 500 msec, which signaled the onset of the trial. After a blank interval of 500 msec, a memory array (simultaneous format) or a memory list (sequential format) consisting of one item (low load) or three items (high load) was presented. For the simultaneous format, the memory array was presented for 450 msec. For the location-sequential and center-sequential formats, each stimulus was presented for 150 msec, with an ISI) of 150 msec. Following

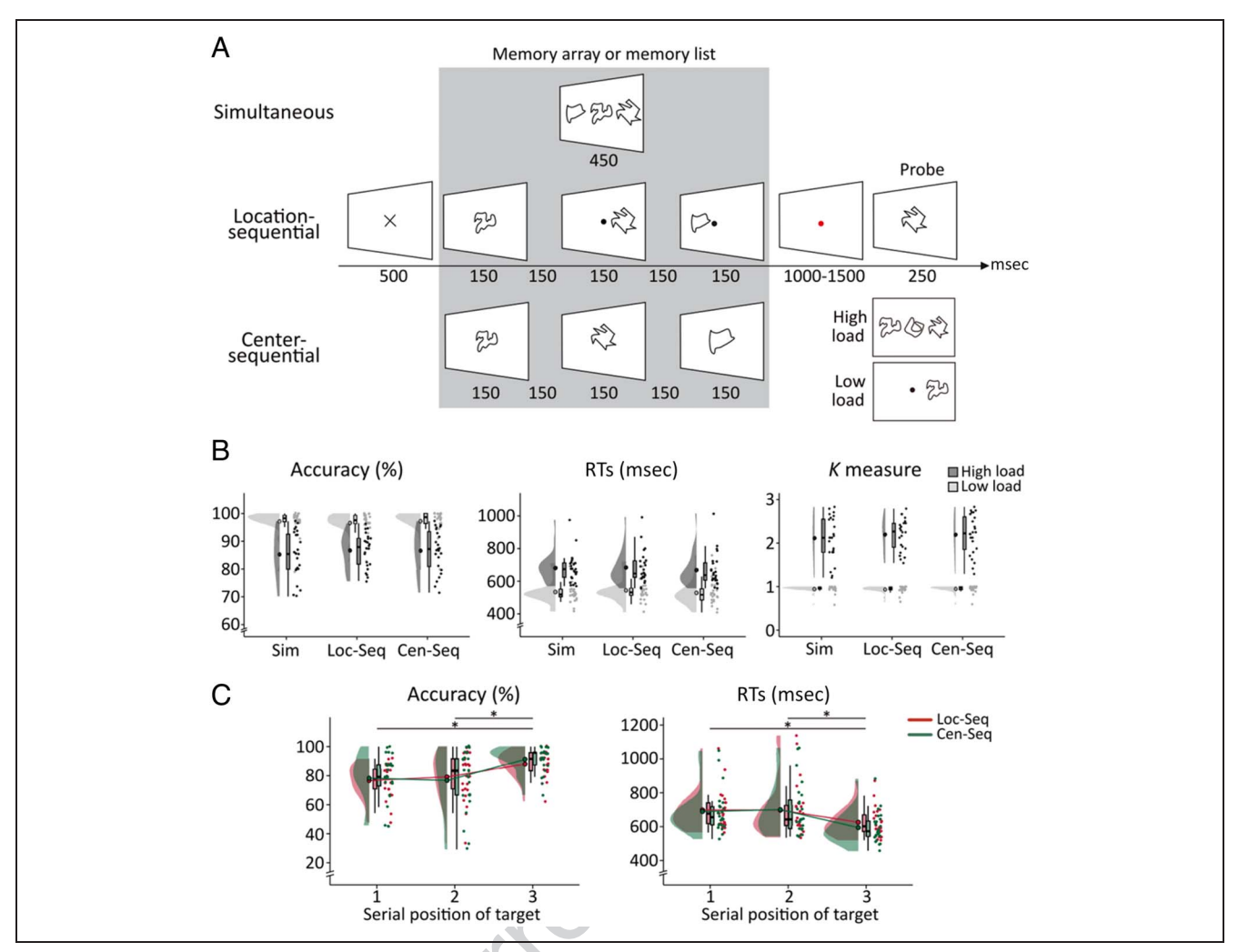


Figure 1. Schematic illustration of WM tasks in simultaneous and sequential presentations and behavioral results. (A) Participants viewed and memorized a memory array (simultaneous presentation) or a memory list (location-sequential and center-sequential presentations) consisting of one item (low load) or three items (high load). Participants were then instructed to indicate whether a probe item was present or absent from the memory array or list. (B) The behavioral results include the mean accuracy (percent correct, %; left panel), RT (msec; middle panel), and capacity measures (K measure; right panel). Sim = simultaneous; Loc-Seq = location-sequential; Cen-Seq = center-sequential. Filled circles in the raincloud plots represent group means, box plots show the median and the 25th and 75th percentiles, and individual dots represent data from each participant. (C) Participants exhibited higher accuracy (left panel) and faster RTs (right panel) when the target was presented in the last (third) position than in the previous two positions in the two sequential presentations. Asterisks indicate significant differences between the target positions (p < .05).

a randomized retention interval (1000–1500 msec, with a red fixation dot), a probe item was presented at the center location for 250 msec. Participants were instructed to indicate whether the probe item was present (50%) or absent (50%) from the memory array or list by pressing the left or right mouse button using their right hand. After the probe disappeared, there was a 1000-msec response window. The intertrial interval (ITI) was 1500–2000 msec. A gray fixation dot was presented at the center of the screen during both ISI and ITI.

Experimental Procedure

The participants sat comfortably in a dimly lit room facing a CRT monitor placed 57 cm in front of them. Prior to the formal experiment, the participants were given written

and verbal instructions about the task requirements. For each presentation format, the participants first completed a practice session of 24 trials to ensure that they could perform the task as instructed. In the formal experiment, the three presentation formats were presented in separate blocks (four blocks for each presentation format), and the order of the blocks was pseudorandom across participants. Trials with different WM loads and response types (target present and target absent) were equiprobable and randomized within each block. There were 12 blocks of 72 trials, yielding 864 trials in total (288 trials for each presentation format). The participants were instructed to maintain fixation on a small fixation marker at the center of the screen during the experimental trials and to respond as quickly and accurately as possible. They were encouraged to rest between blocks that they could self-initiate and were also asked to minimize blinking and movement of their eyes while performing each trial throughout the experiment. The total experimental time for each participant was approximately 120 min.

Behavioral Analyses

Behavioral measures, including accuracy and RT, were analyzed by a 3 (presentation format: simultaneous, location-sequential, and center-sequential) \times 2 (WM load: high, low) repeated-measures ANOVA. Only correct responses were included in the RT analyses. We calculated median RTs for each condition for each participant to reduce the influence of occasional outliers. Additionally, the K measure was calculated using the following equation: K = S (set size of the memory array or memory list) \times (hit rate – false alarm rate) (Cowan, 2001). The hit rate was defined as the conditional probability that the participants responded "target present" when the target was present, and the false alarm rate was defined as the conditional probability that the participants responded "target present" when the target was absent.

Moreover, the recency effect (Murdock, 1962; Deese & Kaufman, 1957) was examined in the two sequential conditions for high WM load. We tested whether accuracy and RTs differed according to the serial position of the target (i.e., the first, second, and third positions) during encoding. Accuracy and RTs were analyzed by a 2 (presentation format: location-sequential and center-sequential) \times 3 (target position: first, second, and third) repeated-measures ANOVA.

EEG Acquisition and Recording Parameters

The EEG data were recorded continuously using a NuAmps amplifier (Neuroscan Inc.) with a 37-electrode elastic cap (Ag/AgCl) arranged according to the 10-20 international system. The montage included six midline sites (FZ, FCZ, CZ, CPZ, PZ, and OZ) and 12 sites over each hemisphere (FP1/FP2, F3/F4, F7/F8, FC3/FC4, FT7/FT8, C3/C4, T3/T4, CP3/CP4, TP7/TP8, P3/P4, T5/T6, and O1/O2). Vertical eye movements were recorded by electrodes placed on the supraorbital and infraorbital ridges of the left eye (vertical EOG [VEOG]), and horizontal eye movements were recorded by electrodes placed on the outer canthi of the right and left eyes (horizontal EOG [HEOG]). The ground and reference electrodes were positioned at AFz (positioned between FPz and Fz) and the mastoid sites (A1 and A2), with A2 serving as the active online reference. Electrode impedances were kept below 5 K Ω throughout the recording. Ongoing EEG signals at each electrode site were sampled at a rate of 1000 Hz. The activity was filtered with a low-pass filter of 100 Hz, and no high-pass filter was used. The stimulus presentation codes for each event were sent to the EEG acquisition computer via a parallel port from the stimulus

presentation computer to indicate the type and exact time of presentation.

EEG Preprocessing

Offline, the continuous EEG signals were re-referenced to the algebraic average of the left and right mastoids (A1 and A2). Bipolar EOG signals were derived by computing the difference between the HEOG and VEOG signals. We epoched the EEG signals based on the onset of memory and probe stimuli separately. For the encoding and maintenance epochs, the continuous data were segmented into epochs starting 3100 msec before and ending 2950 msec after the onset of the memory array in the simultaneous condition or the last stimulus of the memory list in the two sequential conditions. For the probe epochs, the continuous data were segmented into epochs starting 1000 msec before and ending 2500 msec after the onset of the test probe. The encoding and maintenance epochs were baseline-corrected using a 100-msec prestimulus period time-locked to the onset of the last stimulus in the two sequential conditions and to the onset of the memory array in the simultaneous condition. For the probe epochs, baseline correction was applied using a 100-msec prestimulus period time-locked to the onset of the probe stimulus. Epochs containing excessive noise or drift (±100 μV) at any electrode and epochs with eye movement artifacts (blinks or saccades) were excluded. Blinks were identified as large deflections ($\pm 60 \mu V$) in the HEOG or VEOG electrodes. Visual inspection was then performed to confirm the appropriate removal of artifacts and identify residual saccades or eye movements in individual HEOG traces. Trials with incorrect behavioral responses were excluded from further analyses. After preprocessing, the average number of trials per WM load and presentation format was 108.38 ± 18.57 trials out of 144 trials for the encoding/maintenance epochs and 56.87 ± 8.64 trials out of 72 target-present trials for the probe epochs.

WM Encoding and Maintenance: EEG Time-Frequency Analysis

The offline EEG time–frequency analyses were performed using SPM software (Wellcome Centre for Human Neuroimaging, University College London) and the Fieldtrip toolbox (Oostenveld, Fries, Maris, & Schoffelen, 2011) in MATLAB (MathWorks, Inc.) complemented by in-house MATLAB scripts. The EEG signal epochs were downsampled to 250 Hz and spatially filtered by the spherical spline surface Laplacian transformation to reduce the influence of volume conduction (Perrin, Pernier, Bertrand, & Echallier, 1989). The epochs were then subjected to time–frequency decomposition using continuous Morlet wavelet transformation with a length of seven cycles. Time–frequency representations of power were estimated for each trial, electrode, and participant across frequencies

from 1 to 20 Hz in 1-Hz steps. The resulting time–frequency power was averaged across the trials for each presentation format and WM load separately. The power estimates were rescaled to decibels, with a baseline from -400 to -100 msec prior to the onset of the memory array for the simultaneous format or the first stimulus in the memory list for the sequential formats.

Statistical analyses were performed on power estimates across participants using a cluster-based nonparametric permutation approach (Maris & Oostenveld, 2007) and a repeated-measures ANOVA. For the nonparametric permutation test, a dependent-samples t statistic was first computed at each time point across frequencies from 8 to 13 Hz, based on the power estimates averaged over eight predefined posterior electrodes (e.g., P3/Z/4, T5/6 and O1/ $\mathbb{Z}/2$). Samples with p values below the threshold (p < .05, two-tailed) were selected and grouped into clusters based on temporal adjacency. For each cluster, a cluster-level t statistic was computed by summing the t values within the cluster. The cluster with the maximum cluster-level t statistic (the "maxsum" in Fieldtrip) was used for hypothesis testing and computing the corrected p value. Monte Carlo p values were then calculated using 1000 permutations, in which the two conditions were randomly shuffled to generate a null distribution of clusterlevel statistics under the null hypothesis. The observed cluster-level t statistic was compared against this null distribution to obtain a corrected p value. A cluster was considered statistically significant if its p value was less than .05 (two-tailed), indicating that the observed cluster was unlikely to have occurred by chance. This analysis approach effectively controls for Type I errors without making strong prior assumptions about the distribution of the data.

We tested the effect of WM load (high vs. low) during the 1000-msec time window of WM maintenance period after the stimulus offset separately for each presentation format: 450-1450 msec after memory array onset for the simultaneous presentation and 150-1150 msec after the last stimulus onset for the two sequential presentations. We also examined the effect of presentation format by comparing alpha power in two contrasts, separately for each load condition: (1) simultaneous versus locationsequential presentation formats and (2) locationsequential versus center-sequential presentation. The comparison between simultaneous and locationsequential presentation formats was designed to assess the influence of the ordinal information on WM processing (450–1150 msec after memory array onset for the simultaneous presentation and after the last stimulus onset for the location-sequential presentation), as both conditions provided spatial information. In contrast, the comparison between location-sequential and center-sequential presentation formats was designed to assess the influence of spatial information on WM processing, as both conditions included ordinal information. Moreover, we examined the interaction between presentation format and WM load. Load-dependent alpha power differences (high vs. low) were computed for the following presentation format comparisons: (1) simultaneous versus location-sequential and (2) location-sequential versus center-sequential. Importantly, our design allowed us to analyze alpha power across the three stimulus positions in both sequential conditions when WM load was high. Specifically, we compared alpha power differences between the location-sequential and center-sequential conditions during the encoding period (from -600 to 300 msec relative to the onset of the last stimulus) for high-load trials.

In addition to the permutation test, we conducted repeated-measures ANOVA to analyze power estimates during the maintenance and encoding periods separately. First, we extracted the mean alpha power estimates over the parieto-occipital electrodes (e.g., P3/Z/4, T5/6, and O1/Z/2) during the maintenance period from 450 to 1450 msec after the onset of the memory array in the simultaneous condition and from 150 to 1150 msec after the onset the last stimulus in the sequential conditions. We conducted a two-way 3 (presentation format: simultaneous, location-sequential, center-sequential) × 2 (WM load: high, low) repeated-measures ANOVA on these data. This analysis allowed us to examine the effects of presentation format and WM load on alpha power during the maintenance period.

Second, the mean posterior alpha power estimates for each memory stimulus during the encoding period (0-150 msec after each stimulus offset) were extracted for both location-sequential and center-sequential conditions. We conducted a 2 (presentation format: location-sequential, center-sequential) \times 3 (stimulus position: first, second, and third) repeated-measures ANOVA on these data. This analysis allowed us to examine the effects of presentation format and stimulus position on WM encoding.

WM Retrieval: ERP Analysis

For the probe epochs, we conducted ERP analysis to test whether WM load can continue to modulate neural activity across different presentation formats during WM retrieval. The probe epochs were filtered with a low-pass filter of 40 Hz and averaged across trials according to the conditions of interest. We used the N3rs as the neural marker (Kuo et al., 2009; Nobre et al., 2008) and compared the N3rs magnitudes when participants searched retroactively for the target item among three items versus one item in the memory array/list. N3rs was quantified by measuring the mean amplitudes between 300 and 400 msec for the anterior (F3/Z/4 and FC3/Z/4), central (C3/Z/4 and CP3/Z/4), and posterior (P3/Z/4 and O1/Z/2) electrode sites. We conducted a three-way repeated-measures ANOVA to test the effects of presentation format, WM load, and electrode site. This analysis allowed us to examine the effects of presentation format and WM load on the N3rs during WM retrieval.

In addition, we tested whether the magnitude of N3rs can be influenced by the serial position of the target (i.e., the first, second, or third position) for high WM load in the two sequential conditions. To this end, we conducted a four-way repeated-measures ANOVA to test the effects of presentation format (location-sequential and center-sequential), WM load, target position (first, second, and third), and electrode site. For high-load conditions, trials were sorted according to the target position (first, second, and third); for low-load conditions, all trials were based on a single position. This analysis allowed us to examine the effects of presentation format, WM load, and target position on the N3rs during WM retrieval. The Greenhouse-Geisser epsilon correction for nonsphericity was applied to all ERP analyses where appropriate (Jennings & Wood, 1976), and only corrected probability values and degrees of freedom are reported. Bonferroni correction was applied to all post hoc comparisons in the behavioral and EEG/ERP repeated-measures ANOVAs, and adjusted p values are reported.

RESULTS

Behavioral Results

Behavioral results are illustrated in Figure 1. Accuracy data revealed a significant main effect of WM load, F(1, 23) =75.83, p < .001, $\eta_p^2 = .77$, suggesting a higher accuracy for low load (97.00 \pm 4.07%) than for high load (86.16 \pm 6.51%). No other effect on accuracy was significant: the main effect of presentation format, F(2, 46) = 0.62, p =.543, η_p^2 = .03, and the interaction between WM load and presentation format, F(2, 46) = 1.26, p = .294, $\eta_p^2 = .05$. RT data revealed a significant main effect of WM load, $F(1, 23) = 174.09, p < .001, \eta_p^2 = .88$, suggesting faster RTs for low load (535.14 \pm 70.16 msec) than for high load (678.22 \pm 96.61 msec). We also observed a significant main effect of presentation format, F(1.31,30.19) = 4.11, p = .042, η_p^2 = .15, indicating faster RTs for the center-sequential condition (598.58 \pm 85.68 msec) than for the location-sequential condition (613.83 ± 81.91 msec), t(23) = 3.44, p = .007, Cohen's d = 0.70. The interaction between WM load and presentation format was not significant, $F(2, 46) = 0.71, p = .498, \eta_p^2 =$.03. The analyses of WM capacity revealed a significant main effect of WM load, F(1, 23) = 272.57, p < .001, $\eta_{\rm p}^2$ = .92, suggesting greater K measures for high load $(2.17 \pm 0.39 \, K)$ than for low load $(0.94 \pm 0.08 \, K)$. No other effect on WM capacity was significant: the main effect of presentation format, F(2, 46) = 0.75, p = .48, η_p^2 = .03, and the interaction between WM load and presentation format, $F(2, 46) = 0.97, p = .386, \eta_p^2 = .04$.

We further tested for the behavioral recency effect for the two sequential conditions for high load. Accuracy data revealed a significant main effect of target position, F(2,

46) = 13.12, p < .001, $\eta_p^2 = .36$, suggesting a higher accuracy when the target was presented in the last (third) position (89.67% \pm 7.36%) than in the previous two positions (first position: $77.47\% \pm 12.28\%$, second position: 77.95% \pm 17.34%): first versus third position: t(23) = 5.74, p <.001, Cohen's d = 1.17; second versus third position: t(23) = 3.71, p = .003, Cohen's d = 0.76. No other effects on accuracy were significant: the main effect of presentation format, F(1, 23) = 0.24, p = .629, $\eta_p^2 = .01$, and the interaction between position and presentation format, $F(2, 46) = 1.51, p = .231, \eta_p^2 = .06$. RT data also revealed a significant main effect of position, F(1.47, 33.82) = 21.65, p < .001, $\eta_p^2 = .48$, suggesting faster RTs when the target was presented in the last position (609.83 \pm 84.63 msec) than in the previous two positions (first position: $693.73 \pm$ 114.16 msec, second position: 698.70 ± 152.40 msec): first versus third position: t(23) = 6.62, p < .001, Cohen's d =1.35; second versus third position: t(23) = 4.63, p < .001, Cohen's d = 0.95. No other effects on RT were significant: the main effect of presentation format, F(1, 23) = 2.47, p =.129, η_p^2 = .10, and the interaction between position and presentation format, $F(2, 46) = 2.01, p = .146, \eta_p^2 = .08$.

In summary, a significant load effect was observed across all three presentation formats. In addition, participants exhibited longer RTs in the location-sequential condition than in the center-sequential condition, suggesting the influence of spatial information on WM performance. Finally, a recency effect was observed in the two sequential high-load conditions, with higher accuracy and faster RTs when the target was presented in the last position than when it was presented in the previous two positions.

EEG Results

WM Maintenance and Encoding: Time–Frequency Results

The time-frequency results are shown in Figure 2. We first tested for the effect of WM load on alpha power over the posterior electrodes during the retention interval for each presentation format. During the early maintenance stage, significant decreases in alpha power were observed for high load relative to low load for the simultaneous condition from 450 to 1144 msec (corrected p < .001, Cohen's d = 1.17), for the location-sequential condition from 150 to 372 msec (corrected p < .001, Cohen's d = 1.21), and for the center-sequential condition from 150 to 200 msec (corrected p = .02, Cohen's d = 0.59). During the late maintenance stage, significant increases in alpha power were observed for high load relative to low load for the location-sequential condition from 824 to 1150 msec (corrected p = .005, Cohen's d = 0.54) and for the center-sequential condition at 10-12 Hz alpha frequencies from 744 to 902 msec (corrected p = .009, Cohen's d = 0.30) and from 1064 to 1148 msec (corrected p =.021, Cohen's d = 0.35).

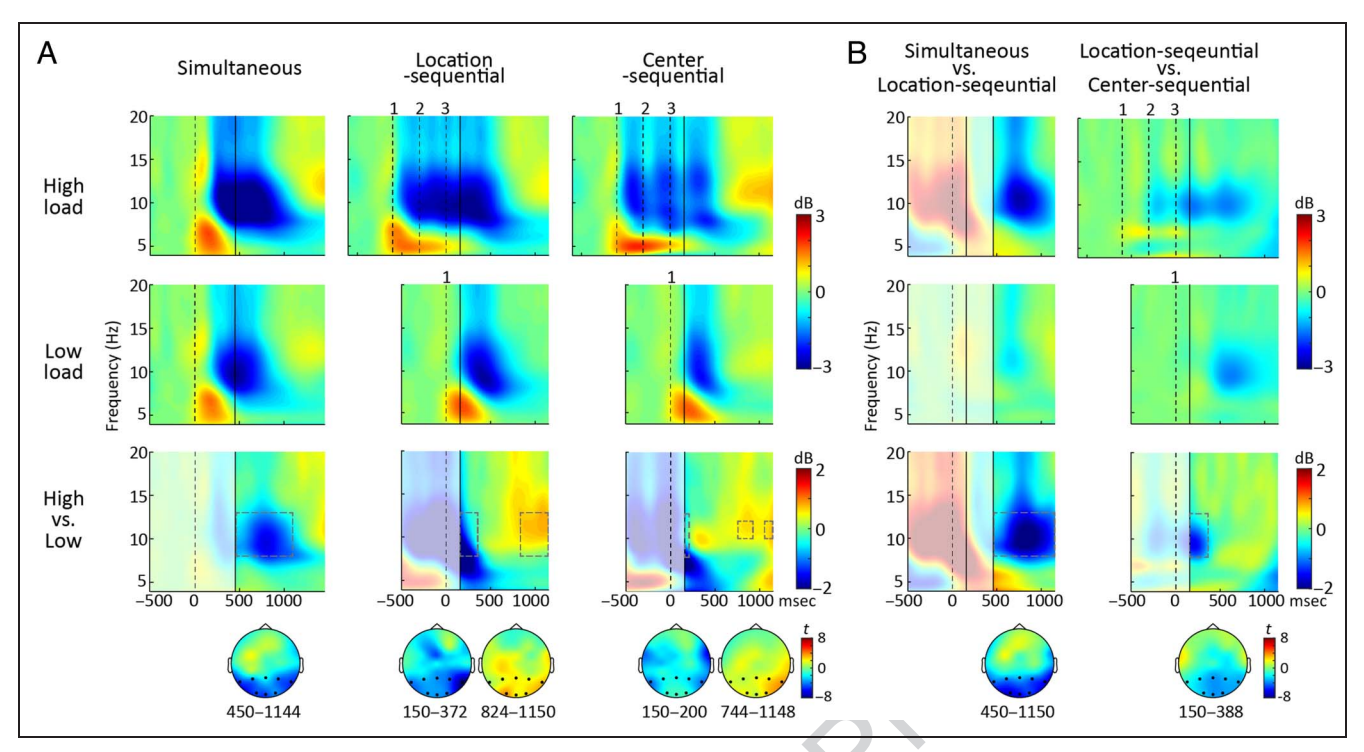


Figure 2. Time–frequency results during WM maintenance and encoding for different presentation formats. (A) When comparing high load versus low load, we found a significant decrease in posterior alpha power throughout WM maintenance in the simultaneous condition and during early WM maintenance in both sequential conditions. We also identified a significant increase in posterior alpha power during late WM maintenance in the two sequential conditions. Numbers 1, 2, and 3 indicate the temporal order of the stimulus position during the sequential presentation. "0 msec" indicates the onset of the memory array in simultaneous presentation and the last stimulus in sequential presentations. The dashed lines on the time–frequency plots indicate the onset of the stimulus, and the solid lines indicate the offset of the memory array in simultaneous presentation and the last stimulus in sequential presentations. Topographical maps (bottom) indicate the significant effects on alpha power (8–13 Hz), and the time windows (msec) are indicated by the dashed-line squares (10–12 Hz for the alpha power increase in the center-sequential presentation). (B) We found a greater decrease in posterior alpha power in the simultaneous condition than in the location-sequential condition than in the center-sequential condition at high and low WM load. We also found a larger load-dependent decrease in alpha power in the simultaneous condition than in the location-sequential condition than in the center-sequential condition.

In addition to the load effect, we also tested the alpha power differences between the presentation formats for each load. At high WM load, greater decreases in alpha power were observed for the simultaneous condition than for the location-sequential condition from 450 to 1150 msec (corrected p < .001, Cohen's d = 1.88) and for the location-sequential condition than for the centersequential condition from 150 to 1096 msec (corrected p < .001), Cohen's d = 1.18. At low WM load, greater decreases in alpha power were observed for the simultaneous condition than for the location-sequential condition from 500 to 832 msec (corrected p = .002, Cohen's d = 0.81) and for the location-sequential condition than for the center-sequential condition from 340 to 1150 msec (corrected p < .001, Cohen's d = 1.29).

Furthermore, we found a significant interaction between presentation format and WM load. Load-dependent alpha power attenuation was greater for the simultaneous condition than for the location-sequential condition from 450 to 1150 msec (corrected p < .001, Cohen's d = 1.55) and for the location-sequential condition than for the center-sequential condition from

150 to 338 msec (corrected p < .001, Cohen's d = 0.95).

Repeated-measures ANOVA was conducted to supplement the permutation tests and revealed a significant interaction effect between the presentation format and WM load on alpha power, F(1.56, 35.89) = 17.47, p < .001, $\eta_p^2 = .43$ (Figure 3). Post hoc comparisons showed a greater reduction in alpha power for high load relative to low load for simultaneous presentations (-0.71 ± 0.90 dB) than for location-sequential presentations (0.01 ± 0.75 dB), t(23) = 5.18, p < .001, Cohen's d = 1.06, and center-sequential presentations (0.15 ± 0.85 dB), t(23) = 4.46, p = .001, Cohen's d = 0.91. This analysis revealed a stronger load-dependent decrease in alpha power for the simultaneous condition compared with both sequential conditions.

In addition to maintenance-related alpha power, we also analyzed alpha power across the three serial positions during the encoding period in both sequential conditions for high WM load (Figure 4). We tested the differences in alpha power between the two sequential presentations across three memory stimuli in the high-load condition.

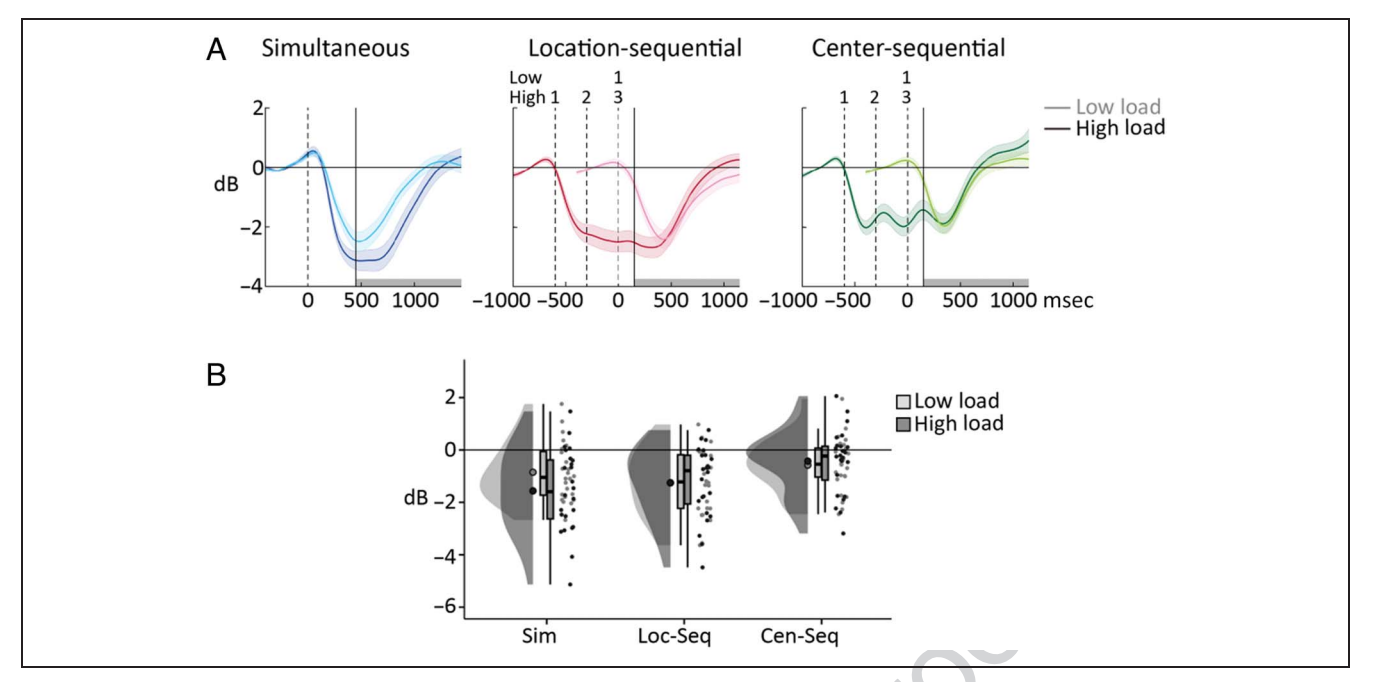
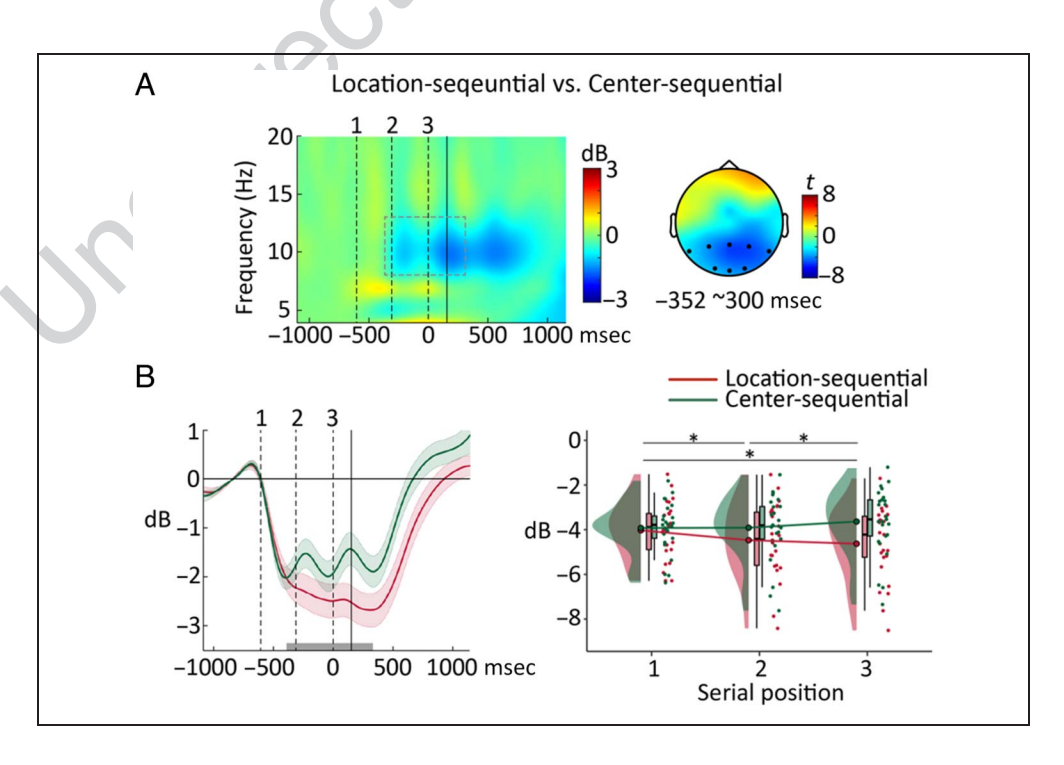


Figure 3. Alpha power (8–13 Hz) during WM maintenance and encoding for different presentation formats. (A) Time courses of alpha power across the posterior electrodes (P3/Z/4, T5/6, and O1/Z/2) are presented for each condition. Numbers 1, 2, and 3 indicate the temporal order of the stimulus position during the sequential presentation. "0 msec" indicates the onset of the last stimulus. The dashed lines in the plots indicate the onset of each stimulus, and the solid lines indicate the offset of the last stimulus. Shaded areas represent the *SEM*. The gray line indicates the time window of interest. (B) Posterior alpha power during 1000-msec WM maintenance showed a greater load-dependent decrease in alpha power in the simultaneous condition (Sim) than in the location-sequential (Loc-Seq) and center-sequential (Cen-Seq) conditions. Filled circles in the raincloud plots represent group means, box plots show the median and the 25th and 75th percentiles, and individual dots represent data from each participant.

Figure 4. Time-frequency results during the encoding period for the two sequential conditions. (A) We found a greater decrease in alpha power for the location-sequential condition than for the centersequential condition during the encoding period. Numbers 1, 2, and 3 indicate the temporal order of the stimulus position during the sequential presentation. "0 msec" indicates the last stimulus onset. The topographical map indicates the significant effect on alpha power, and the time window is indicated by the dashed-line square. (B) EEG data demonstrated a consecutive decrease in alpha power with the presentation of each additional item in the locationsequential condition but not in the center-sequential condition (left panel). Shaded areas represent the SEM. The gray



line indicates the time window of interest. The dashed lines in the plots indicate the onset of each stimulus, and the solid lines indicate the offset of the last stimulus. A greater decrease in alpha power was found in the location-sequential condition than in the center-sequential condition for the second position compared with the first position and for the third position compared with the second position and the first position (right panel). Filled circles in the raincloud plots represent group means, box plots show the median and the 25th and 75th percentiles, and individual dots represent data from each participant. Asterisks indicate significant differences (p < .05).

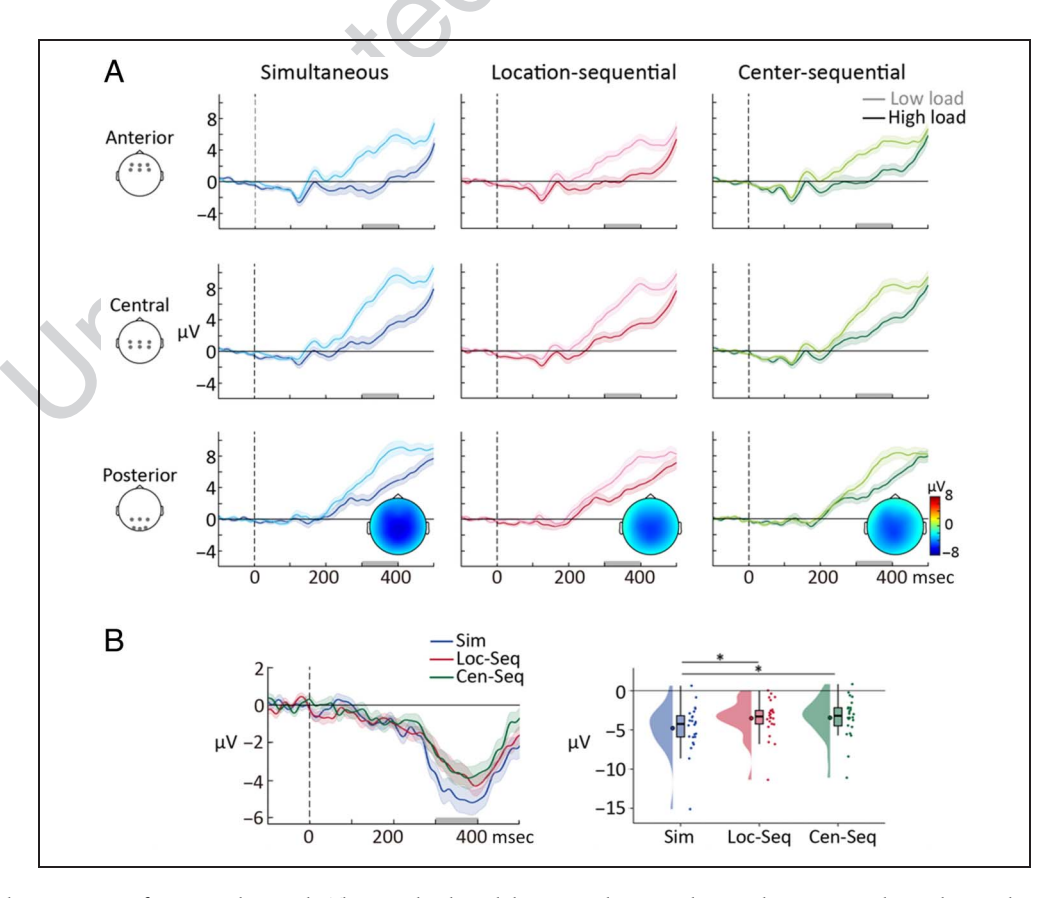
First, the permutation test showed a greater decrease in alpha power for the location-sequential condition than for the center-sequential condition from -352 to 300 msec relative to the last stimulus onset (corrected p < .001, Cohen's d = 1.06). The repeated-measures ANOVA further revealed a significant interaction between presentation format and serial position, $F(2, 46) = 20.65, p < .001, \eta_p^2 =$.47. Post hoc analysis showed that the alpha power decrease for the location-sequential condition relative to the centersequential condition was greater for the second position $(-0.56 \pm 0.63 \text{ dB})$ than for the first position $(-0.10 \pm$ 0.42 dB), t(23) = 4.11, p = .001, Cohen's d = 0.84, and for the third position (-0.99 ± 0.94 dB) than for the second position, t(23) = 3.94, p = .002, Cohen's d = 0.80, and the first position, t(23) = 4.90, p < .001, Cohen's d = 0.89. Post hoc analysis also revealed a greater decrease in alpha power for the second position relative to the first position $(-0.44 \pm 0.68 \text{ dB}), t(23) = 3.20, p = .012, \text{ Cohen's } d =$ 0.65, and for the third position relative to the first position $(-0.60 \pm 0.85 \text{ dB}), t(23) = 3.43, p = .007, \text{ Cohen's } d =$ 0.70, in the location-sequential condition. However, no significant difference was observed among the three positions in the center-sequential condition, F(1.46, 35.12) = 3.25, p =.065, $\eta_p^2 = 0.12$.

WM Retrieval: ERP Results

The N3rs results for different presentation formats are shown in Figure 5, and only the effects with WM load were of interest. We first tested the effect of N3rs on WM load, $F(1, 23) = 65.01, p < .001, \eta_p^2 = .74$, which revealed that the amplitudes were more negative for high load (2.00 \pm 2.32 μ V) than for low load (5.92 \pm 2.95 μ V) across the three WM tasks. The interaction effect between presentation format and WM load was significant, F(1, 96, 44.99) =5.50, p = .008, $\eta_p^2 = .19$, reflecting a stronger N3rs load modulation in the simultaneous presentation ($-4.78 \pm$ 3.05 μ V) compared with the location-sequential (-3.51 \pm $2.43 \mu V$), t(23) = -2.68, p = .040, Cohen's d = -0.55, and center-sequential ($-3.45 \pm 2.58 \,\mu\text{V}$) presentations, t(23) = -3.18, p = .013, Cohen's d = -0.65. The interaction effect between electrode sites and WM load was also significant, $F(1.33, 30.62) = 13.18, p < .001, \eta_p^2 =$.36, reflecting a stronger N3rs load modulation for the anterior $(-4.13 \pm 2.29 \,\mu\text{V})$ than for the posterior electrodes $(-3.10 \pm 2.49 \,\mu\text{V})$, t(23) = -2.78, p = .032, Cohen's d = -0.56, and for the central $(-4.51 \pm 2.73 \,\mu\text{V})$ than for the posterior electrodes, t(23) = -6.14, p < .001, Cohen's d = -1.25.

Figure 5. ERP results during WM retrieval. (A) The N3rs effect was elicited after the probe onset across the anterior, central, and posterior electrode sites, with more negative amplitudes for high load (darkcolored lines) than for low load (light-colored lines). Grandaveraged waveforms are shown for each presentation format and load. "0 msec" indicates the probe onset. Shaded areas represent the SEM. The gray line represents the time window of interest (300-400 msec). The topographical map indicates the N3rs load modulation (high load minus low load) within the time window. (B) ERP differences between high and low WM load for each presentation format (Sim = simultaneous; Loc-Seq = location-sequential; Cen-Seq = center-sequential) are shown. Waveforms were averaged across anterior, central, and posterior electrodes (left panel). Mean amplitudes were computed for

300-400 msec and averaged



across the same electrodes for each presentation format (right panel). The N3rs load modulation was larger in the simultaneous condition than in the sequential conditions. Filled circles in the raincloud plots represent group means, box plots show the median and the 25th and 75th percentiles, individual dots represent data from each participant. Asterisks indicate significant differences (p < .05).

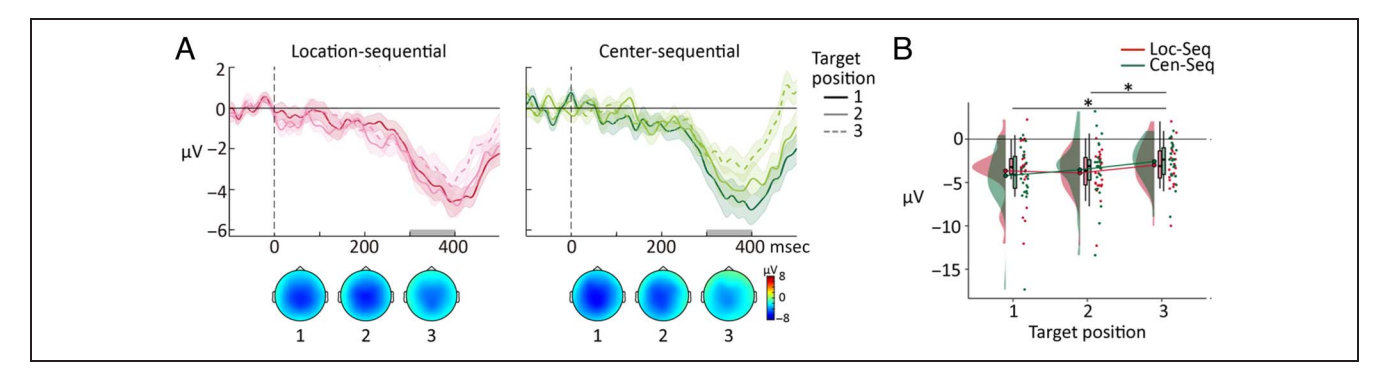


Figure 6. ERP differences between high and low WM load for each target position in the sequential conditions during WM retrieval. (A) Waveforms were averaged across anterior, central and posterior electrodes. "0 msec" indicates the probe onset. Shaded areas represent the SEM. The gray line represents the time window of interest (300–400 msec). The topographical map indicates the N3rs load modulation (high load minus low load) within this time window for each target position. (B) Mean amplitudes were computed for 300–400 msec and averaged across the same electrodes for each target position. A smaller N3rs effect was observed when the target was presented in the last position than in the previous two positions. Filled circles in the raincloud plots represent group means, box plots show the median and the 25th and 75th percentiles, and individual dots represent data from each participant. Asterisks indicate significant differences (p < .05).

Finally, we investigated whether the position of the target modulates the magnitude of the N3rs, and only the effects related to WM load and the target position in the two sequential conditions were of interest (Figure 6). We observed a significant interaction between target position and WM load, $F(1.85, 42.62) = 4.80, p = .015, \eta_p^2 = .17$. This interaction indicated a smaller N3rs effect when the target was presented in the third position $(-2.79 \pm 1.94 \, \mu\text{V})$ relative to the first $(-3.93 \pm 2.97 \, \mu\text{V})$, t(23) = -2.59, p = .049, Cohen's d = -0.53, and the second $(-3.71 \pm 2.64 \, \mu\text{V})$, t(23) = -2.63, p = .045, Cohen's d = -0.54, positions in sequential presentations.

DISCUSSION

WM involves multiple stages of information processing in distributed cortical networks (Christophel et al., 2017; D'Esposito & Postle, 2015; Jonides et al., 2008). Ample evidence has revealed the neural substrates (Sreenivasan & D'Esposito, 2019) and electrophysiological correlates of WM load and capacity during maintenance, particularly in tasks using simultaneous presentations, such as change detection or delay response tasks (Pavlov & Kotchoubey, 2021; Luria et al., 2016). Extending this line of research, we investigated whether and how the presentation format influences electrophysiological responses across WM processes. EEG data were recorded while participants performed WM tasks involving simultaneous, locationsequential, and center-sequential presentations with varying WM loads. Our findings revealed significant variations in alpha power not only during maintenance but also encoding, as well as in N3rs amplitudes during retrieval, depending on presentation formats and WM loads. Taken together, our results showed that presentation formats modulate load-dependent neural responses across all stages of WM processing.

Influence of Presentation Formats during WM Maintenance

Consistent with prior EEG findings (Chen et al., 2022; Fukuda et al., 2015), we observed a persistent decrease in posterior alpha power when comparing high WM load with low WM load for simultaneous presentation. Moreover, our EEG results demonstrated distinct neural dynamics in the load-dependent modulation of alpha power for both sequential presentations, showing an early decrease in alpha power followed by a later increase, as reported in previous research (Bahramisharif, Jensen, Jacobs, & Lisman, 2018). The distinct characteristics of the alpha oscillations during early and late periods imply separate mechanisms involved in WM maintenance depending on the presentation format.

Our findings characterized distinct temporal profiles of alpha-band activity between the simultaneous and sequential presentations. When the memory items were presented simultaneously in an array, all the items were integrated with their locations from encoding through maintenance (Theeuwes, Kramer, & Irwin, 2011; Treisman & Zhang, 2006; Olson & Marshuetz, 2005; Jiang, Olson, & Chun, 2000). The greater decrease in alpha power for high load than low load during maintenance in the simultaneous condition represents the sustained maintenance of memory contents (Chen et al., 2022). Moreover, compared with the center-sequential condition, the location-sequential condition showed a greater decrease in load-dependent alpha power during early maintenance, as this presentation introduces additional spatial information. These findings suggest the heightened engagement of posterior brain regions to sustain sensory representations of memory items, especially when they are bound to spatial locations, during WM maintenance. Our findings were also consistent with previous studies showing that spatial representations can be coded through alpha activity during WM maintenance (Foster, Bsales, Jaffe, & Awh, 2017; Foster, Sutterer, Serences, Vogel, & Awh, 2016).

In contrast, when the memory items were presented sequentially in a memory list, they were integrated with their temporal order from encoding through maintenance (Pomper et al., 2019; Trübutschek, Marti, & Dehaene, 2019). In both sequential conditions, we observed a load-dependent decrease in alpha power during the early maintenance stage, followed by a load-dependent increase during the late maintenance stage. Increases in alpha power during maintenance as the WM load increases have been observed in many WM studies using a modified Sternberg paradigm (Proskovec, Heinrichs-Graham, & Wilson, 2019; Tuladhar et al., 2007; Jensen, Gelfand, Kounios, & Lisman, 2002). This load-dependent increase in alpha power was hypothesized to be related to the functional inhibition of irrelevant information (Klimesch, Sauseng, & Hanslmayr, 2007) or the suppression of task-irrelevant brain areas (Jensen & Mazaheri, 2010). In our study, we propose that the sequential presentations, by providing temporal order information, may have encouraged the use of verbal strategies to facilitate the transmission of sensory input from early to deeper levels of processing (Brady & Störmer, 2022; Pavlov & Kotchoubey, 2021; van Ede, 2018). These strategies may also have helped protect memory lists from external interference as maintenance progressed, consistent with the observed increase in alpha power during the late maintenance stage. The transmission and protection of information can also be supported by the distributed network activity that underlies the selection and maintenance of temporal order information in WM (Johnson, Sutterer, Acheson, Lewis-Peacock, & Postle, 2011; Palva & Palva, 2007).

Taken together, our findings suggest that the maintenance process involves not only the retention of memory content but also top-down modulation to organize and prioritize information according to the presentation format. Alpha oscillations are multifaceted (Clayton, Yeung, & Cohen Kadosh, 2018), shifting between excitatory and inhibitory modes depending on the presentation format. These results reflect the dynamic and representational states during WM maintenance (de Vries, Slagter, & Olivers, 2020).

Influence of Sequential Presentation during Encoding

Beyond maintenance, our EEG data revealed a significant interaction between presentation format and serial position during sequential encoding. Prior research has demonstrated that the magnitude of contralateral delay activity during WM encoding increases with each additional stimulus when memory items are presented sequentially (Pomper et al., 2019; Wang et al., 2019). This cumulative ERP effect reflects the additive effects of WM storage during sequential presentations.

In our study, we observed a consecutive decrease in posterior alpha power with the presentation of additional items in the location-sequential condition during WM encoding for high WM load. Conversely, no successive decrease was found in the center-sequential condition, where alpha power attenuation remained consistent across serial positions. The consecutive alpha power decreases observed in the location-sequential condition likely reflect the accumulation of spatial information across items. These results suggest stronger engagement of visual processing during sequential encoding when spatial information is present (location-sequential condition) compared with when it is absent (center-sequential condition), spanning both encoding and maintenance phases. Nevertheless, these findings should be interpreted with caution, particularly given the subtle differences in stimulus presentation between the two sequential conditions during encoding.

Influence of Presentation Formats during WM Retrieval

The presentation of a probe item during WM retrieval elicited a load-dependent negative potential over midline electrodes approximately 300 msec after probe onset, known as the N3rs. This ERP is hypothesized to reflect retroactive search and internal evaluation of potential targets and competing nontargets within maintained information during retrieval (Kuo, Nobre, Scerif, & Astle, 2016; Kuo et al., 2009; Nobre et al., 2008).

Our ERP results replicated earlier findings, showing a significant N3rs load modulation during WM retrieval in the simultaneous condition. Extending these findings, we also observed significant N3rs load modulations in both sequential conditions, indicating load-dependent activity when searching for the target among sequentially presented items during WM retrieval. Moreover, the N3rs amplitudes varied with presentation formats and target positions, with stronger amplitudes in simultaneous presentation than in sequential presentations and in earlier stimulus positions than in the last position in sequential presentations. Our results suggest that searching for a target item in the simultaneous condition and earlier positions of the sequential conditions required more extensive evaluations of target and nontarget competition from the maintained information. In contrast, targets in the last serial position of the memory list were accessed more easily (Morrison, Conway, & Chein, 2014; Nee & Jonides, 2011; McElree, 2006), contributing to the recency effect (Monsell, 1978; Sternberg, 1969). To our knowledge, this study is the first to demonstrate that presentation formats continue to shape WM retrieval processes, as reflected by the N3rs.

One may wonder whether the N3rs may also reflect the transformation of sensory information into a decision-making process, as indexed by the ERP known as the central parietal positivity (CPP). For example, an early EEG

study measured the CPP in a gradual target detection task in which participants continuously viewed a flickering annulus and detected intermittent reductions in contrast (O'connell, Dockree, & Kelly, 2012). The study found that CPP amplitudes increased steadily with accumulating evidence and peaked at the time of response execution. More recently, an EEG study demonstrated a similar neural decision signal supporting WM-guided behavior in the absence of external sensory input (van Ede & Nobre, 2024). In that study, participants performed a WM task requiring delayed orientation reproduction, and the CPP was observed when participants made decisions based on internally maintained information. In contrast to these studies in which the CPP was time-locked to response onset and reflected a gradual accumulation of external or internal evidence, the N3rs in our study was time-locked to the onset of target-present probes (Nobre et al., 2008). The relationship between retroactive search, as indexed by the N3rs, and gradual decision processes, as indexed by the CPP, during WM retrieval remains an open question. Future studies should investigate these WM-related processes by tracking N3rs and CPP while systematically manipulating decision evidence across varying WM loads.

Implications for Encoding Strategies

In the present study, we observed a robust load effect on behavioral performance across all three presentation formats, with no significant differences among them. These behavioral results are consistent with recent research suggesting that although simultaneous and sequential presentations may favor distinct encoding strategies, they share a similar bottleneck in WM capacity (Zhao & Vogel, 2023). By using EEG, we demonstrated that presentation formats distinctly influenced neural responses across various WM processes. Our EEG results revealed how different presentation formats promote distinct encoding strategies in WM tasks: Simultaneous presentations may encourage spatial encoding, whereas sequential presentations may encourage temporal encoding (Manohar et al., 2017). Recent studies have proposed that sequential presentations facilitate an "each-item-at-once" strategy that increases memory for meaningful objects, whereas simultaneous presentations support a "take-a-snap-shot" strategy that favors simple or unrecognizable objects (Chung et al., 2024; Brady & Störmer, 2022; Asp, Störmer, & Brady, 2021; Brady, Störmer, & Alvarez, 2016). Future research may consider exploring different encoding strategies using real-world or meaningful objects to gain deeper insights into their neural correlates across WM stages.

A limitation of the present study is the imbalance in sensory input between low-load (one item) and high-load (three items) trials. This imbalance may introduce a potential confound of a rebound effect (Tuladhar et al., 2007; Jensen et al., 2002)—a transient increase in alpha power following visual stimulation. Some studies have equated perceptual input by adding task-irrelevant stimuli (i.e.,

fillers) to low-load conditions (Chen et al., 2022; Jensen et al., 2002); however, this approach can also create strategic differences, particularly in sequential presentations where participants might anticipate the target's location. To minimize such confounds and ensure comparability across conditions, we presented only task-relevant stimuli. Importantly, the observed load-dependent attenuation of alpha power in the simultaneous condition replicated previous findings both with fillers (Chen et al., 2022) and without fillers (Fukuda et al., 2015), supporting the robustness of our design. In the simultaneous condition, alpha power decreased during maintenance and gradually returned to baseline for both WM loads, with a larger late increase toward the end of the maintenance period for high load. Because retention intervals were jittered and this late increase in alpha power overlapped with probe onset, it cannot be conclusively interpreted as a rebound effect.

Conclusion

In conclusion, our results provide novel evidence that the spatial and ordinal information embedded in presentation formats modulates load-dependent neural responses across WM processes. Importantly, these effects extend beyond maintenance to include encoding and retrieval processes, highlighting the influence of stimulus presentation formats on changes in neural responses over different stages of WM processing.

Corresponding author: Bo-Cheng Kuo, Department of Psychology, National Taiwan University, No. 1, Sec. 4, Roosevelt Road, 10617, Taipei, Taiwan, e-mail: bckuo@ntu.edu.tw.

Data Availability Statement

All data and materials will be made publicly available following the article's acceptance and research ethics approval.

Author Contribution

Ya-Ting Chen: Conceptualization; Data curation; Formal analysis; Investigation; Methodology; Writing—Original draft; Writing—Review & editing. Bo-Cheng Kuo: Conceptualization; Funding acquisition; Investigation; Methodology; Project administration; Resources; Software; Supervision; Validation; Writing—Original draft; Writing—Review & editing.

Funding Information

This work was supported by grants from the Ministry of Science and Technology (https://dx.doi.org/10.13039/501100004663) (MOST 110-2410-H-002-129-MY3) and the National Science and Technology Council (https://dx.doi.org/10.13039/501100020950) (NSTC 113-2410-H-002-253-MY3), Taiwan, to B.-C. K.

Diversity in Citation Practices

Retrospective analysis of the citations in every article published in this journal from 2010 to 2021 reveals a persistent pattern of gender imbalance: Although the proportions of authorship teams (categorized by estimated gender identification of first author/last author) publishing in the *Journal of Cognitive Neuroscience* (*JoCN*) during this period were M(an)/M = .407, W(oman)/M = .32, M/W = .115, and W/W = .159, the comparable proportions for the articles that these authorship teams cited were M/M = .549, W/M = .257, M/W = .109, and W/W = .085 (Postle and Fulvio, *JoCN*, 34:1, pp. 1–3). Consequently, *JoCN* encourages all authors to consider gender balance explicitly when selecting which articles to cite and gives them the opportunity to report their article's gender citation balance.

REFERENCES

- Asp, I. E., Störmer, V. S., & Brady, T. F. (2021). Greater visual working memory capacity for visually matched stimuli when they are perceived as meaningful. *Journal of Cognitive Neuroscience*, *33*, 902–918. https://doi.org/10.1162/jocn_a 01693, PubMed: 34449847
- Baddeley, A. D. (1992). Working memory. *Science*, *255*, 556–559. https://doi.org/10.1126/science.1736359, PubMed: 1736359
- Bahramisharif, A., Jensen, O., Jacobs, J., & Lisman, J. (2018). Serial representation of items during working memory maintenance at letter-selective cortical sites. *PLOS Biology*, *16*, e2003805. https://doi.org/10.1371/journal.pbio.2003805, PubMed: 30110320
- Bengson, J. J., & Luck, S. J. (2016). Effects of strategy on visual working memory capacity. *Psychonomic Bulletin & Review*, 23, 265–270. https://doi.org/10.3758/s13423-015-0891-7, PubMed: 26139356
- Bettencourt, K. C., & Xu, Y. (2016). Decoding the content of visual short-term memory under distraction in occipital and parietal areas. *Nature Neuroscience*, *19*, 150–157. https://doi.org/10.1038/nn.4174, PubMed: 26595654
- Brady, T. F., & Störmer, V. S. (2022). The role of meaning in visual working memory: Real-world objects, but not simple features, benefit from deeper processing. *Journal of Experimental Psychology: Learning, Memory, and Cognition*, 48, 942–958. https://doi.org/10.1037/xlm0001014, PubMed: 33764123
- Brady, T. F., Störmer, V. S., & Alvarez, G. A. (2016). Working memory is not fixed-capacity: More active storage capacity for real-world objects than for simple stimuli. *Proceedings of the National Academy of Sciences, U.S.A.*, 113, 7459–7464. https://doi.org/10.1073/pnas.1520027113, PubMed: 27325767
- Campbell, J. I. D., & Thompson, V. A. (2012). MorePower 6.0 for ANOVA with relational confidence intervals and Bayesian analysis. *Behavior Research Methods*, 44, 1255–1265. https://doi.org/10.3758/s13428-012-0186-0, PubMed: 22437511
- Chen, Y.-T., van Ede, F., & Kuo, B.-C. (2022). Alpha oscillations track content-specific working memory capacity. *Journal of Neuroscience*, 42, 7285–7293. https://doi.org/10.1523/jneurosci.2296-21.2022, PubMed: 35995565
- Christophel, T. B., Hebart, M. N., & Haynes, J.-D. (2012). Decoding the contents of visual short-term memory from human visual and parietal cortex. *Journal of Neuroscience*,

- 32, 12983–12989. https://doi.org/10.1523/jneurosci.0184-12 .2012, PubMed: 22993415
- Christophel, T. B., Klink, P. C., Spitzer, B., Roelfsema, P. R., & Haynes, J.-D. (2017). The distributed nature of working memory. *Trends in Cognitive Sciences*, *21*, 111–124. https://doi.org/10.1016/j.tics.2016.12.007, PubMed: 28063661
- Chung, Y. H., Brady, T. F., & Störmer, V. S. (2024). Sequential encoding aids working memory for meaningful objects' identities but not for their colors. *Memory and Cognition*, 52, 2119–2131. https://doi.org/10.3758/s13421-023-01486-4, PubMed: 37948024
- Clayton, M. S., Yeung, N., & Cohen Kadosh, R. (2018). The many characters of visual alpha oscillations. *European Journal of Neuroscience*, 48, 2498–2508. https://doi.org/10.1111/ejn.13747, PubMed: 29044823
- Cowan, N. (1998). Attention and memory: An integrated framework. Oxford, United Kingdom: Oxford University Press. https://doi.org/10.1093/acprof:oso/9780195119107.001 0001
- Cowan, N. (2001). The magical number 4 in short-term memory: A reconsideration of mental storage capacity. *Behavioral and Brain Sciences*, 24, 87–114. https://doi.org/10.1017/s0140525x01003922, PubMed: 11515286
- Deese, J., & Kaufman, R. A. (1957). Serial effects in recall of unorganized and sequentially organized verbal material. *Journal of Experimental Psychology*, 54, 180–187. https://doi.org/10.1037/h0040536, PubMed: 13475644
- D'Esposito, M. (2007). From cognitive to neural models of working memory. *Philosophical Transactions of the Royal Society of London, Series B: Biological Sciences*, *362*, 761–772. https://doi.org/10.1098/rstb.2007.2086, PubMed: 17400538
- D'Esposito, M., & Postle, B. R. (2015). The cognitive neuroscience of working memory. *Annual Review of Psychology*, 66, 115–142. https://doi.org/10.1146/annurev-psych-010814-015031, PubMed: 25251486
- de Vries, I. E. J., Slagter, H. A., & Olivers, C. N. L. (2020).

 Oscillatory control over representational states in working memory. *Trends in Cognitive Sciences*, 24, 150–162. https://doi.org/10.1016/j.tics.2019.11.006, PubMed: 31791896
- Endo, N., Saiki, J., Nakao, Y., & Saito, H. (2003). Perceptual judgments of novel contour shapes and hierarchical descriptions of geometrical properties. *Shinrigaku Kenkyu: The Japanese Journal of Psychology*, 74, 346–353. https://doi. org/10.4992/jjpsy.74.346, PubMed: 14708480
- Foster, J. J., Bsales, E. M., Jaffe, R. J., & Awh, E. (2017). Alphaband activity reveals spontaneous representations of spatial position in visual working memory. *Current Biology*, 27, 3216–3223. https://doi.org/10.1016/j.cub.2017.09.031, PubMed: 29033335
- Foster, J. J., Sutterer, D. W., Serences, J. T., Vogel, E. K., & Awh, E. (2016). The topography of alpha-band activity tracks the content of spatial working memory. *Journal of Neurophysiology*, 115, 168–177. https://doi.org/10.1152/jn.00860.2015, PubMed: 26467522
- Frick, R. W. (1985). Testing visual short-term memory: Simultaneous versus sequential presentations. *Memory and Cognition*, *13*, 346–356. https://doi.org/10.3758/BF03202502, PubMed: 4079750
- Fukuda, K., Mance, I., & Vogel, E. K. (2015). α power modulation and event-related slow wave provide dissociable correlates of visual working memory. *Journal of Neuroscience*, *35*, 14009–14016. https://doi.org/10.1523
- Harrison, S. A., & Tong, F. (2009). Decoding reveals the contents of visual working memory in early visual areas. *Nature*, 458, 632–635. https://doi.org/10.1038/nature07832, PubMed: 19225460

- Jensen, O., Gelfand, J., Kounios, J., & Lisman, J. E. (2002). Oscillations in the alpha band (9–12 Hz) increase with memory load during retention in a short-term memory task. *Cerebral Cortex*, 12, 877–882. https://doi.org/10.1093/cercor/12.8.877, PubMed: 12122036
- Jensen, O., & Mazaheri, A. (2010). Shaping functional architecture by oscillatory alpha activity: Gating by inhibition. Frontiers in Human Neuroscience, 4, 186. https://doi.org/10.3389/fnhum.2010.00186, PubMed: 21119777
- Jiang, Y. V., Olson, I. R., & Chun, M. M. (2000). Organization of visual short-term memory. *Journal of Experimental Psychology: Learning, Memory, & Cognition*, 26, 683–702. https://doi.org/10.1037/0278-7393.26.3.683, PubMed: 10855426
- Johnson, J. S., Sutterer, D. W., Acheson, D. J., Lewis-Peacock, J. A., & Postle, B. R. (2011). Increased alpha-band power during the retention of shapes and shape-location associations in visual short-term memory. *Frontiers in Psychology*, 2, 128. https://doi.org/10.3389/fpsyg.2011.00128, PubMed: 21713012
- Jonides, J., Lewis, R. L., Nee, D. E., Lustig, C. A., Berman, M. G., & Moore, K. S. (2008). The mind and brain of short-term memory. *Annual Review of Psychology*, 59, 193–224. https:// doi.org/10.1146/annurev.psych.59.103006.093615, PubMed: 17854286
- Klimesch, W., Sauseng, P., & Hanslmayr, S. (2007). EEG alpha oscillations: The inhibition-timing hypothesis. *Brain Research Reviews*, *53*, 63–88. https://doi.org/10.1016/j.brainresrev.2006.06.003, PubMed: 16887192
- Kuo, B.-C., Nobre, A. C., Scerif, G., & Astle, D. E. (2016). Top-down activation of spatiotopic sensory codes in perceptual and working memory search. *Journal of Cognitive Neuroscience*, 28, 996–1009. https://doi.org/10.1162/jocn_a_00952, PubMed: 26967943
- Kuo, B.-C., Rao, A., Lepsien, J., & Nobre, A. C. (2009). Searching for targets within the spatial layout of visual short-term memory. *Journal of Neuroscience*, 29, 8032–8038. https://doi.org/10.1523/JNEUROSCI.0952-09.2009, PubMed: 19553443
- Linke, A. C., Vicente-Grabovetsky, A., Mitchell, D. J., & Cusack, R. (2011). Encoding strategy accounts for individual differences in change detection measures of VSTM. Neuropsychologia, 49, 1476–1486. https://doi.org/10.1016/j.neuropsychologia.2010.11.034, PubMed: 21130789
- Luck, S. J., & Vogel, E. K. (2013). Visual working memory capacity: From psychophysics and neurobiology to individual differences. *Trends in Cognitive Sciences*, 17, 391–400. https://doi.org/10.1016/j.tics.2013.06.006, PubMed: 23850263
- Luria, R., Balaban, H., Awh, E., & Vogel, E. K. (2016). The contralateral delay activity as a neural measure of visual working memory. *Neuroscience & Biobehavioral Reviews*, 62, 100–108. https://doi.org/10.1016/j.neubiorev.2016.01.003, PubMed: 26802451
- Manohar, S. G., Pertzov, Y., & Husain, M. (2017). Short-term memory for spatial, sequential and duration information. *Current Opinion of Behavioral Science*, 17, 20–26. https://doi.org/10.1016/j.cobeha.2017.05.023, PubMed: 29167809
- Maris, E., & Oostenveld, R. (2007). Nonparametric statistical testing of EEG- and MEG-data. *Journal of Neuroscience Methods*, *164*, 177–190. https://doi.org/10.1016/j.jneumeth .2007.03.024, PubMed: 17517438
- McElree, B. (2006). Accessing recent events. *Psychology of Learning and Motivation*, 46, 155–200. https://doi.org/10.1016/S0079-7421(06)46005-9
- Miyake, A., & Shah, P. (1999). *Models of working memory: Mechanisms of active maintenance and executive control.*Cambridge, United Kingdom: Cambridge University Press.
 https://doi.org/10.1017/CBO9781139174909

- Monsell, S. (1978). Recency, immediate recognition memory, and reaction time. *Cognitive Psychology*, *10*, 465–501. https://doi.org/10.1016/0010-0285(78)90008-7
- Morrison, A. B., Conway, A. R. A., & Chein, J. M. (2014). Primacy and recency effects as indices of the focus of attention. *Frontiers in Human Neuroscience*, 8, 6. https://doi.org/10.3389/fnhum.2014.00006, PubMed: 24478672
- Murdock, B. B., Jr. (1962). The serial position effect of free recall. *Journal of Experimental Psychology*, 64, 482. https://doi.org/10.1037/h0045106
- Nee, D. E., & Jonides, J. (2011). Dissociable contributions of prefrontal cortex and the hippocampus to short-term memory: Evidence for a 3-state model of memory. *Neuroimage*, 54, 1540–1548. https://doi.org/10.1016/j .neuroimage.2010.09.002, PubMed: 20832478
- Nobre, A. C., Griffin, I. C., & Rao, A. (2008). Spatial attention can bias search in visual short-term memory. *Frontiers in Human Neuroscience*, *1*, 4. https://doi.org/10.3389/neuro.09.004.2007, PubMed: 18958218
- O'connell, R. G., Dockree, P. M., & Kelly, S. P. (2012). A supramodal accumulation-to-bound signal that determines perceptual decisions in humans. *Nature Neuroscience*, *15*, 1729–1735. https://doi.org/10.1038/nn.3248, PubMed: 23103963
- Okuhata, S., Kusanagi, T., & Kobayashi, T. (2013). Parietal EEG alpha suppression time of memory retrieval reflects memory load while the alpha power of memory maintenance is a composite of the visual process according to simultaneous and successive Sternberg memory tasks. *Neuroscience Letters*, 555, 79–84. https://doi.org/10.1016/j.neulet.2013.09 .010, PubMed: 24036459
- Oldfield, R. (1971). Edinburgh handedness inventory. *Journal of Abnormal Psychology*. https://doi.org/10.1037/t23111-000
- Olson, I. R., & Marshuetz, C. (2005). Remembering "what" brings along "where" in visual working memory. *Perception & Psychophysics*, 67, 185–194. https://doi.org/10.3758/bf03206483, PubMed: 15971683
- Oostenveld, R., Fries, P., Maris, E., & Schoffelen, J.-M. (2011). FieldTrip: Open source software for advanced analysis of MEG, EEG, and invasive electrophysiological data. *Computational Intelligence and Neuroscience*, 2011, 156869. https://doi.org/10.1155/2011/156869, PubMed: 21253357
- Palva, S., & Palva, J. M. (2007). New vistas for α-frequency band oscillations. *Trends in Neurosciences*, *30*, 150–158. https://doi.org/10.1016/j.tins.2007.02.001, PubMed: 17307258
- Pavlov, Y. G., & Kotchoubey, B. (2021). Oscillatory brain activity and maintenance of verbal and visual working memory: A systematic review. *Psychophysiology*, 59, e13735. https://doi .org/10.1111/psyp.13735, PubMed: 33278030
- Perrin, F., Pernier, J., Bertrand, O., & Echallier, J. F. (1989). Spherical splines for scalp potential and current density mapping. *Electroencephalography and Clinical Neurophysiology*, 72, 184–187. https://doi.org/10.1016/0013 -4694(89)90180-6, PubMed: 2464490
- Pomper, U., Ditye, T., & Ansorge, U. (2019). Contralateral delay activity during temporal order memory. *Neuropsychologia*, 129, 104–116. https://doi.org/10.1016/j.neuropsychologia .2019.03.012, PubMed: 30922830
- Proskovec, A. L., Heinrichs-Graham, E., & Wilson, T. W. (2019). Load modulates the alpha and beta oscillatory dynamics serving verbal working memory. *Neuroimage*, 184, 256–265. https://doi.org/10.1016/j.neuroimage.2018.09.022, PubMed: 30213775
- Serences, J. T. (2016). Neural mechanisms of information storage in visual short-term memory. Vision Research, 128, 53–67. https://doi.org/10.1016/j.visres.2016.09.010, PubMed: 27668990

- Serences, J. T., Ester, E. F., Vogel, E. K., & Awh, E. (2009). Stimulus-specific delay activity in human primary visual cortex. *Psychological Science*, *20*, 207–214. https://doi.org/10.1111/j.1467-9280.2009.02276.x, PubMed: 19170936
- Sreenivasan, K. K., & D'Esposito, M. (2019). The what, where and how of delay activity. *Nature Reviews Neuroscience*, 20, 466–481. https://doi.org/10.1038/s41583-019-0176-7, PubMed: 31086326
- Sternberg, S. (1969). Memory-scanning: Mental processes revealed by reaction-time experiments. *American Scientist*, *57*, 421–457. PubMed: 5360276
- Stokes, M. G. (2015). 'Activity-silent' working memory in prefrontal cortex: A dynamic coding framework. *Trends in Cognitive Sciences*, *19*, 394–405. https://doi.org/10.1016/j.tics.2015.05.004, PubMed: 26051384
- Theeuwes, J., Kramer, A. F., & Irwin, D. E. (2011). Attention on our mind: The role of spatial attention in visual working memory. *Acta Psychologia*, *137*, 248–251. https://doi.org/10.1016/j.actpsy.2010.06.011, PubMed: 20637448
- Todd, J. J., & Marois, R. (2004). Capacity limit of visual short-term memory in human posterior parietal cortex. *Nature*, 428, 751–754. https://doi.org/10.1038/nature02466, PubMed: 15085133
- Treisman, A., & Zhang, W. (2006). Location and binding in visual working memory. *Memory and Cognition*, *34*, 1704–1719. https://doi.org/10.3758/BF03195932, PubMed: 17489296
- Trübutschek, D., Marti, S., & Dehaene, S. (2019). Temporal-order information can be maintained in non-conscious working memory. *Scientific Reports*, *9*, 6484. https://doi.org/10.1038/s41598-019-42942-z, PubMed: 31019199
- Tuladhar, A. M., Huurne, N., Schoffelen, J.-M., Maris, E., Oostenveld, R., & Jensen, O. (2007). Parieto-occipital sources account for the increase in alpha activity with working memory load. *Human Brain Mapping*, *28*, 785–792. https://doi.org/10.1002/hbm.20306, PubMed: 17266103

- Unsworth, N. (2016). Working memory capacity and recall from long-term memory: Examining the influences of encoding strategies, study time allocation, search efficiency, and monitoring abilities. *Journal of Experimental Psychology: Learning, Memory, and Cognition*, 42, 50–61. https://doi.org/10.1037/xlm0000148, PubMed: 26076331
- van Ede, F. (2018). Mnemonic and attentional roles for states of attenuated alpha oscillations in perceptual working memory: A review. *European Journal of Neuroscience*, 48, 2509–2515. https://doi.org/10.1111/ejn.13759, PubMed: 29068095
- van Ede, F., & Nobre, A. C. (2024). A neural decision signal during internal sampling from working memory in humans. *Journal of Neuroscience*, 44, e1475232024. https://doi.org/10.1523/JNEUROSCI.1475-23.2024, PubMed: 38538144
- Vogel, E. K., & Machizawa, M. G. (2004). Neural activity predicts individual differences in visual working memory capacity. *Nature*, 428, 748–751. https://doi.org/10.1038/nature02447, PubMed: 15085132
- Vogel, E. K., McCollough, A. W., & Machizawa, M. G. (2005). Neural measures reveal individual differences in controlling access to working memory. *Nature*, 438, 500–503. https://doi.org/10.1038/nature04171, PubMed: 16306992
- Wang, S., Rajsic, J., & Woodman, G. F. (2019). The contralateral delay activity tracks the sequential loading of objects into visual working memory, unlike lateralized alpha oscillations. *Journal of Cognitive Neuroscience*, *31*, 1689–1698. https://doi.org/10.1162/jocn a 01446, PubMed: 31274391
- Xu, Y. (2017). Reevaluating the sensory account of visual working memory storage. *Trends in Cognitive Sciences*, 21, 794–815. https://doi.org/10.1016/j.tics.2017.06.013, PubMed: 28774684
- Zhao, C., & Vogel, E. K. (2023). Sequential encoding paradigm reliably captures the individual differences from a simultaneous visual working memory task. *Attention*, *Perception*, & *Psychophysics*, 85, 366–376. https://doi.org/10.3758/s13414-022-02647-4, PubMed: 36624199